

Exploring Hybrid Active and Passive Multiple Access via Slotted ALOHA-Driven Backscatter Communications

Bowen Gu, Hao Xie, Dong Li, *Senior Member, IEEE*, Ye Liu, Yongjun Xu, *Senior Member, IEEE*

Abstract—In conventional backscatter communication (BackCom) systems, various centralized access schemes, i.e., time division multiple access (TDMA) and frequency division multiple access (FDMA), are generally adopted for multi-user backscattering to avoid transmission collisions. However, as the number of backscatter devices (BDs) proliferates, there will be high overhead, and more seriously, the proactive inter-user coordination is unaffordable for the passive BDs, which are of scarce concern in existing works and remain a challenge to solve. To this end, in this paper, we leverage a slotted ALOHA (SA)-based random access for multi-BD BackCom systems, in which each BD is randomly chosen and is allowed to coexist with one active device for hybrid active and passive transmission. To excavate and evaluate the performance, a resource allocation problem for max-min average throughput is formulated, where transmit antenna selection, receive beamforming design, reflection coefficient (RC) adjustment, power control, and access probability determination are jointly optimized. To deal with this intractable problem, we first transform the objective function with the max-min form into an equivalent linear one, and then decompose the resulting problem into three sub-problems. Next, a block coordinate descent (BCD)-based greedy algorithm with maximum ratio combining (MRC), semi-definite programming (SDP), and variable substitution is designed to obtain the sub-optimal solution. Besides, we derive the closed-form solutions for RC and transmit power for tractable analysis. Simulation results demonstrate that the proposed algorithm outperforms benchmark algorithms in terms of throughput and fairness.

Index Terms—Backscatter communications, hybrid active and passive transmission, random access, resource allocation

I. INTRODUCTION

As massive wireless devices are continuously connected to the Internet, the development of human society has been moved from the period of information revolution represented by the Internet to the period of intelligent revolution represented by the Internet of Things (IoT), heralding the opening of the door to the Internet of Everything [1]–[3]. By 2024, a forecast shows that the number of IoT devices will reach 83 billion, which will be a powerful contributor to making everything connected [4]. However, the other side of the coin is that worries have multiplied about how to supply power

to such huge amounts of IoT devices in light of the current energy poverty and the non-negligible energy consumption of each device [5]. As a result, it is an urgent matter to reduce the energy consumption of IoT devices.

Backscatter communication (BackCom), as a cost-, spectrum-, and energy-efficient communication technology, promises to alleviate the power-hungry issue [6]. Specifically, wireless devices can adjust the reflection coefficient (RC) by changing the impedance, thus reflecting and modulating the incident radio-frequency (RF) signal from a dedicated signal source without the carrier signal generated by oscillators. Thus, it avoids demodulation and decoding, and requires no additional RF components, which prompts the circuit power consumption of BackCom several orders of magnitude less than that of conventional communications. Along with the evolution of BackCom, ambient backscatter communication (AmBack) inherits the hallmarks of BackCom, and differs from the former in that AmBack is allowed to utilize the surrounding RF sources or systems like cellular base stations (BSs), digital television transmitters, Wi-Fi access points, frequency modulation (FM) signals, LoRa signals, and Bluetooth signals [7].

A. Related Works

However, in the AmBack/BackCom system, it cannot be overlooked that, the backscattered signal undergoes double-channel fading, which is to blame for the vulnerable signal at the receiver. In other words, both the signals from other backscatter devices (BDs) (i.e., backscattering links) and from the RF source (i.e., direct link (DL)) interfere with the current backscattering signal, leading to significant degradation in signal detection and transmission performance. Therefore, it is hard to overstate the importance to reduce the impacts of interference and improve the transmission performance for the AmBack/BackCom. In particular, to circumvent the destruction on backscattering transmission imposed by the DL interference (DLI), interference subtraction [8] and opportunistic successive interference cancellation (SIC) [9] have been applied to the AmBack/BackCom as pivotal techniques to deal with the DLI issue. On the other hand, to create an interference-free environment in multi-BD scenarios, time division multiple access (TDMA) has been widely applied in the AmBack/BackCom to avoid the interference generated by concurrent transmission among BDs, in which each BD was allowed to backscatter information by turns [10]–[12]. Besides, the frequency shift (FS) has been also widely adopted to mitigate the mutual interference (MI) among BDs and

Bowen Gu, Hao Xie, and Dong Li are with the Faculty of Information Technology, Macau University of Science and Technology, Avenida Wai Long, Taipa, Macau 999078, China (e-mails: 21098538ii30001@student.must.edu.mo, 3220005631@student.must.edu.mo, dli@must.edu.mo).

Ye Liu is with the School of Computer Science and Engineering, Macau University of Science and Technology, Avenida Wai Long, Taipa, Macau 999078, China, and also with the College of Artificial Intelligence, Nanjing Agricultural University, Nanjing 210031, China (e-mail: yeliu@njau.edu.cn).

Yongjun Xu is with the School of Communication and Information Engineering, Chongqing University of Posts and Telecommunications, Chongqing 400065, China (e-mails: xuyj@cqupt.edu.cn).

TABLE I
SUMMARY OF THE RELATED LITERATURE FOR BACKCOMS WITH RESOURCE ALLOCATION.

Ref.	Network type	BD number	Optimization criterion	Multiple access	Cooperative transmission	Fairness	Non-linear EH	DLI cancellation	MI cancellation	Random control
[9]	SISO	Single	Outage probability	N/A	N/A	N/A	✗	✓ (SIC)	N/A	✗
[10]	MIMO	Multiple	Energy efficiency	TDMA	N/A	✗	✓	✓ (SIC)	✓ (TDMA)	✗
[11]	SISO	Multiple	Energy efficiency	TDMA	N/A	✓	✓	✓ (SIC)	✓(TDMA)	✗
[12]	SISO	Multiple	Achievable throughput	TDMA	N/A	✓	✗	✗	✓ (TDMA)	✗
[13]	SISO	Multiple	Revenue	FDMA	N/A	✗	N/A	✓ (FS)	✓ (FS)	✗
[14]	SISO	Multiple	Ergodic capacity	FDMA	N/A	✗	✗	✓ (FS)	✓ (FS)	✗
[16]	SISO	Single	Ergodic capacity	N/A	Hybrid mode	N/A	✗	N/A	N/A	✗
[17]	MISO	Single	Symbol error rate	N/A	Hybrid mode	N/A	N/A	✓ (SIC)	N/A	✗
[18]	SISO	Multiple	Computation delay	TDMA	Hybrid mode	✓	✓	✓ (SIC)	✓ (TDMA)	✗
[19]	SISO	Single	Ergodic capacity	N/A	Hybrid access	N/A	✗	✓ (SIC)	N/A	✗
[20]	SISO	Single	System capacity	N/A	Hybrid access	N/A	✗	✓ (SIC)	N/A	✗
[21]	SISO	Single	SNR	N/A	Hybrid access	N/A	✗	✓ (MMSE)	N/A	✗
[30]	SISO	Multiple	SINR	OFDM RCMA	Hybrid access	✓	✓	✓ (SIC)	✗	✓
Our work	SIMO	Multiple	Average throughput	SA	Hybrid access	✓	✓	✓ (SIC)	✓ (SA)	✓

DLI so that the DL signal and backscattering signals can be shifted to the non-overlapping frequency bands for interference avoidance [13]–[15].

Another dark cloud hanging overhead is conventional AmBack/BackCom systems rely heavily on dedicated or surrounding energy sources to carry tag signals for backscattering. However, it is not always available to obtain such dedicated energy sources and the surrounding energy signals may not be always stable. One possible solution to circumvent these problems is to allow passive BDs to coexist with traditional active users/systems to share the same spectrum. There have been already some works regarding hybrid active and passive nodes in the spectrum sharing scenarios for cooperative transmission. In [16]–[18], the BD was incorporated into traditional active transmitter devices so that the adaptive switch between the active and passive mode selection is made possible. By integrating both active and passive devices for spectrum sharing, the system performance can be guaranteed but without any additional transmit power or channel bandwidth resources. In [19]–[21], the spectrum sharing between active and passive devices was considered, where the active devices (ADs) served as energy sources for BDs, and BDs were responsible for protecting the ADs from harmful interference similar to the principle of cognitive radio.

B. Motivations and Contributions

It can be seen from the works mentioned above that the traditional centralized access schemes, i.e., TDMA and FDMA, are generally adopted in multi-BD AmBack/BackCom systems to avoid the MI among BDs. However, in view of the proliferating number of IoT devices, is it cost-effective enough to maintain these centralized access schemes? On

the one hand, such centralized access schemes are achieved through an organized and predetermined approach, which requires coordination among sources. However, it may be unaffordable for such simple passive devices to coordinate with each other proactively. On the other hand, a central controller may assist in deconflicting this situation. However, there is an essential prerequisite that the BS perfectly knows all channel information without the overhead, or a small number of devices is involved for optimization. It can be foreseen that the result is pessimistic, which may be well-meaning but ineffectual and overstretched. Thus, it is necessary to explore an access protocol for BackComs with a low overhead and a low complexity.

With this in mind, random access has recently been revisited and regarded as a vital technology for the medium access control (MAC) layer of massive IoT [22]. Random access has unique benefits, such as low latency for small payload transmission, no initial connection setup, no dedicated resource allocation for connection maintenance, and no signaling overhead for radio resource allocation. Among them, the slotted ALOHA (SA) is indisputably one of the finest protocols for random access, which avoids collisions due to partially overlapping transmissions, while retaining low complexity. It is worth mentioning that the revival of the SA has become a promising trend and received attention in various application scenarios, including, e.g., non-orthogonal multiple access-based systems [23], unmanned aerial vehicle-based systems [24], satellite networks [25], wireless-powered communication networks [26]–[29], etc.

Motivated by the above observations, in this paper, we concentrate on investigating the BackCom system performance with the hybrid active and passive multiple access, in which

one AD and multiple BDs are able to share the same radio spectrum to transmit information to the receiver cooperatively. Besides, incorporating the SA into the multi-BD BackCom system is also one of the centerpieces, in which each BD is accessed by obeying an independent probability. To our knowledge, this is the first time that SA is exploited in favour of BDs' access control, belonging to a decentralized and random access scheme, in contrast to the existing works using centralized access schemes, such as, TDMA (see, e.g., [10]–[12], [18]) and FDMA (see, e.g., [13]–[15]). By virtue of its peculiarity, the BackCom system can not only eschew the coordination among passive devices, but also effectively avoid the MI. Although a random code-based multiple access (RCMA) was involved in [30], in which each BD could precode its data by multiplying with a random spreading code and backscatter the incident signal, so that the need of the coordination among BDs could also be avoided. However, this work ignores the issue of poor decoding performance caused by the concurrent transmission among multiple BDs, which is in contrast to our work. For more visualization, Table I briefly summarizes the differences between this paper and the mentioned works. Besides, unlike traditional BS, for a battery-constrained AD, its limited power supply and computing capability may not be able to handle overly complex transmit beamforming computations and the energy consumption associated with multiple antenna operations. In order to circumvent these issues, the transmit antenna selection (TAS) is adopted to reduce the power budget and the computation complexity.

In a nutshell, the main contributions of this paper are summarized as follows:

- To excavate and evaluate the performance of the hybrid active and passive multiple access-based BackCom system with the SA, an optimization problem for maximizing the average throughput is formulated via joint TAS, beamforming design, RC adjustment, power control, and access probability determination, where both the non-linearity of EH and the transmission fairness among BDs are taken into account. Besides, the quality-of-service (QoS) support of the AD is also accommodated for benign cooperation. However, the resulting problem is non-convex and challenging to solve.
- To surmount the obstacles posed by the formulated problem, we first transform its objective function with the max-min form into an equivalent linear one by using a slack variable and decompose the resulting problem into three sub-problems. Then, a block coordinate descent (BCD)-based greedy algorithm with maximum ratio combining (MRC), semi-definite programming (SDP), and variable substitution is proposed to obtain the sub-optimal solution. It is worth pointing out that the closed-form solutions of the receive beamforming of the backscattering signal, the RC, and the transmit power are derived for analytical insights.
- Simulation results demonstrate that the proposed algorithm has good convergence and outperforms benchmark algorithms in terms of transmission performance and fairness by evaluating the impact of network parameters,

TABLE II
ABBREVIATIONS

Notation	Meaning
AD	Active device
AmBack	Ambient backscatter
AP	Access point
AWGN	Additive Gaussian white noise
BackCom	Backscatter communication
BCD	Block coordinate descent
BD	Backscatter devise
BS	Base station
CAP	Channel access probability
CSCG	Circularly symmetric complex Gaussian
DL	Direct link
DLI	Direct-link interference
ECAP	Equal channel access probability
EH	Energy harvesting
FDMA	Frequency division multiple access
FRC	Fixed reflection coefficient
FS	Frequency shift
IoT	Internet of Things
MAC	Medium access control
MI	Mutual interference
MIMO	Multiple input multiple output
MISO	Multiple input single output
MRC	Maximum ratio combining
MMSE	Minimum-mean-square-error
PSD	Positive semi-definite
QoS	Quality-of-service
RC	Reflection coefficient
RCMA	Random code-based multiple access
RF	Radio frequency
RTAS	Random transmit antenna selection
SA	Slotted ALOHA
SIC	Successive interference cancellation
SINR	Signal-to-interference-plus-noise ratio
SIMO	Single input multiple output
SISO	Single input single output
SDP	Semi-definite Programming
SNR	Signal-to-noise ratio
TA	Transmit antenna
TAS	Transmit antenna selection
TDMA	Time division multiple access

such as the maximum transmit power, the number of receive antennas, the number of BDs, the noise power, and the minimum achievable throughput on the performance of the different algorithms. Furthermore, we identify specific conditions under which the performance of low-complexity benchmark algorithms can approximate that of the proposed algorithm, providing a useful shortcut for practical applications.

C. Organization and Notations

The remainder of the paper is organized as follows: In Section II, we present the system model and formulate an

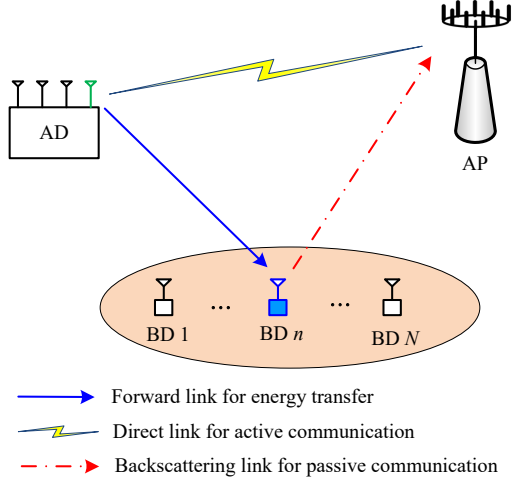


Fig. 1. An uplink BackCom system with multiple BDs.

optimization problem. In Section III, a BCD-based algorithm is proposed to solve the formulated problem. Section IV gives the simulation results, and Section V concludes this paper.

Throughout the paper, scalars, vectors, and matrices are denoted by lowercase, boldface lowercase, and boldface uppercase letters, respectively. $|\cdot|$ and $\|\cdot\|$ denote the absolute value of a complex scalar and the l_2 -norm of a vector, respectively. $(\cdot)^H$, $\text{Rank}(\cdot)$, and $\text{Tr}(\cdot)$ represent the Hermitian, the rank, and the trace of the matrix, respectively. $\delta_i(\cdot)$ denotes the i -th largest singular value of the matrix. \mathbf{I}_K represents the $K \times K$ identity matrix. $\mathbb{E}[\cdot]$ is the statistical expectation. $\mathcal{CN}(\mu, \sigma^2)$ is the circularly symmetric complex Gaussian (CSCG) distribution with mean μ and variance σ^2 . $[\cdot]^+ = \max(0, \cdot)$ denotes the non-negative value. The abbreviations in this paper are summarized in Table II.

II. SYSTEM MODEL AND PROBLEM FORMULATION

A. Network Architecture and Access Protocol

We consider an uplink BackCom system, as shown in Fig. 1, which consists of one AD with M transmit antennas (TAs) (i.e., $m \in \mathcal{M} = \{1, 2, \dots, M\}$), N single-antenna BDs (i.e., $n \in \mathcal{N} = \{1, 2, \dots, N\}$), and one access point (AP) with K receive antennas (i.e., $k \in \mathcal{K} = \{1, 2, \dots, K\}$). Specifically, the AD preserves connecting with the AP actively, while N BDs are able to backscatter information in a passive manner, which are cooperating with the AD. To reduce the computation complexity, a TAS scheme is applied at the AD, in which only one TA can be selected to transmit information at one slot. Having regard to BDs belonging to passive devices, which cannot be colluded in advance, the SA is utilized to control the access of BDs. Assuming that channels between the transmitter and the receiver follow a block-fading model, namely, the corresponding channel gains remain constant for at least one time interval [31]. Each BD is assumed to always have information to send, in the corresponding transmission duration, the decision of the n -th BD on whether to access the channel is determined by the outcome of a Bernoulli experiment, modeled by a random variable $I_n \in \{0, 1\}$, which is realized locally at the n -th BD [28]. When $I_n = 1$ holds,

	Access Status (is it accessed at the current slot?)		
BD 1	Yes	No	No
...	No	No	No
BD n	Yes	Yes	No
...	No	No	No
BD N	Yes	No	No
Transmission Status	Collision	Success	Idleness

Fig. 2. An access schematic of BDs with the SA.

the n -th BD transmits information, and it is silent otherwise, i.e.,

$$I_n = \begin{cases} 1, & \text{with probability } q_n, \\ 0, & \text{with probability } 1 - q_n, \end{cases} \quad (1)$$

where $\mathbb{E}[I_n] = q_n$, $\mathbb{E}[1 - I_n] = 1 - q_n$, and q_n is the channel access probability (CAP) of the n -th BD.

It is noted that only one BD can be accessed at the same time to avoid the MI. For the sake of visualization, Fig. 2 is provided. Specifically, a transmission collision will occur when two or more BDs transmit information at the same time, and it is regarded as successful transmission only and only if there is only one BD is accessed to backscatter its information. Accordingly, the successful CAP of the n -th BD is equal to $\Pr(n) = q_n \prod_{j \neq n} (1 - q_j)$.

B. Non-linear Energy Harvesting

When the m -th TA of the AD is selected, the received signal at the n -th BD can be expressed as

$$y_{m,n}^{\text{BD}} = \sqrt{P_m} h_{m,n}^f s_m + z_n, \forall m, n, \quad (2)$$

where s_m is transmitted symbol by the m -th TA of the AD, satisfied $\mathbb{E}(|s_m|^2) = 1$. P_m denotes the transmit power of the m -th TA of the AD. $h_{m,n}^f$ denotes the channel coefficient from the m -th TA of the AD to the n -th BD. $z_n \sim \mathcal{CN}(0, \sigma_n^2)$ is the additive Gaussian white noise (AWGN), and σ_n^2 denotes the noise power at the n -th BD.

It is worth stating that since each BD is passive, its received signal needs to be divided into two parts, one to serve the communication demands and the other to serve as an energy signal for its circuit operation. Besides, the noise is too weak for energy harvesting (EH) and can be ignored. Thus, based on (2), the harvested power for the operation support of the n -th BD from the m -th TA can be expressed as

$$P_n^{\text{EH}} = (1 - \alpha_n) \sum_{m=1}^M \beta_m P_m |h_{m,n}^f|^2, \forall n, \quad (3)$$

where α_n is the RC of the n -th BD. β_m denotes the TA selection (TAS) factor, i.e., when the m -th TA is selected, $\beta_m = 1$; otherwise, $\beta_m = 0$.

Extensive studies have demonstrated that wireless EH is a nonlinear process that is influenced by the maximum saturation as well as the minimum sensitivity of the device's energy

harvester (see, i.e., [11] and [32]). To avoid resource mismatch, a non-linear EH model is employed, and thus the harvested energy of the n -th BD can be expressed as

$$\begin{aligned} & \Phi_n(P_n^{\text{EH}}) \\ &= \left[\frac{P_n^{\text{SA}}}{\exp(-a_n P_n^{\text{SE}} + b_n)} \left\{ 1 + \exp(-a_n P_n^{\text{SE}} + b_n) - 1 \right\} \right]^+, \forall n \end{aligned} \quad (4)$$

where $\Phi_n(P_n^{\text{EH}})$ is the actual power that can be harvested by the n -th BD. P_n^{SA} and P_n^{SE} denote the thresholds of EH saturation and the EH sensitivity for the n -th BD, respectively. Moreover, a_n and b_n are constants that can control the steepness of $\Phi_n(P_n^{\text{EH}})$.

C. Active and Passive Transmission

When the m -th TA of the AD is selected and the n -th BD is accessed, the received hybrid active and passive signals at the AP can be expressed as

$$\mathbf{y}_{m,n}^{\text{AP}} = \underbrace{\sqrt{P_m} \mathbf{h}_m^{\text{d}} s_m}_{\text{active link}} + \underbrace{\sqrt{\alpha_n P_m} h_{m,n}^{\text{f}} \mathbf{h}_n^{\text{b}} s_m c_n}_{\text{passive link}} + \mathbf{z}_{\text{AP}}, \forall m, n, \quad (5)$$

where c_n is the transmitted symbol by the n -th BD, satisfying $\mathbb{E}(|c_n|^2) = 1$. $\mathbf{h}_m^{\text{d}} \in \mathbb{C}^{K \times 1}$ and $\mathbf{h}_n^{\text{b}} \in \mathbb{C}^{K \times 1}$ denote the channel vectors of the m -th TA-AP link and the BD n -AP link, respectively. $\mathbf{z}_{\text{AP}} \in \mathbb{C}^{K \times 1}$ denotes the noise vector of the AP and is assumed to be a circularly symmetric complex Gaussian (CSCG) random vector with $\mathbf{w}^{\text{R}} \sim \mathcal{CN}(0, \sigma_w^2 \mathbf{I}_K)$. σ_w^2 denotes the noise power.

Recall that the backscattering signal undergoes double-path loss, which leads to the signal strength of the backscattering link being much weaker than that of the DL. As a result, the AP can first decode the DL signal from $\mathbf{y}_{m,n}^{\text{AP}}$ via SIC, then cancels out the decoded signal from $\mathbf{y}_{m,n}^{\text{AP}}$, and finally detects the backscattering signal c_n . Hereinafter, we let $\mathbf{v}_{m,n}^{\text{A}} \in \mathbb{C}^{K \times 1}$ and $\mathbf{v}_{m,n}^{\text{B}} \in \mathbb{C}^{K \times 1}$, respectively, denote the linear receive beamforming employed at the AP for detecting the active signal and the backscattering signal of the n -th BD, and $\mathbf{v}_{m,n} \triangleq [\mathbf{v}_{m,n}^{\text{A}}, \mathbf{v}_{m,n}^{\text{B}}]$. By adopting the receive beamforming, the active signal received by the AP can be expressed as

$$\begin{aligned} \mathbf{y}_{m,n}^{\text{AP}} &= (\mathbf{v}_{m,n}^{\text{A}})^{\text{H}} \mathbf{y}_{m,n}^{\text{AP}} \\ &= (\mathbf{v}_{m,n}^{\text{A}})^{\text{H}} \sqrt{P_m} \mathbf{h}_m^{\text{d}} s_m + \sqrt{\alpha_n P_m} h_{m,n}^{\text{f}} (\mathbf{v}_{m,n}^{\text{A}})^{\text{H}} \mathbf{h}_n^{\text{b}} s_m c_n \\ &\quad + (\mathbf{v}_{m,n}^{\text{A}})^{\text{H}} \mathbf{z}_{\text{AP}}, \forall m, n. \end{aligned} \quad (6)$$

It is noted that, when decoding the DL signal, the backscattering signal is regarded as the interference. Thus, the signal-to-interference-plus-noise ratio (SINR) of the AD with the m -th TA and the n -th BD is given by

$$\gamma_{m,n}^{\text{AD}} = \frac{|(\mathbf{v}_{m,n}^{\text{A}})^{\text{H}} \mathbf{h}_m^{\text{d}}|^2 P_m}{\alpha_n |h_{m,n}^{\text{f}}|^2 |(\mathbf{v}_{m,n}^{\text{A}})^{\text{H}} \mathbf{h}_n^{\text{b}}|^2 P_m + \sigma_w^2}, \forall m, n. \quad (7)$$

The system transmission time slot is normalized to 1. Accordingly, the achievable throughput of the AD when the

n -th BD accesses the channel is expressed as

$$R_n^{\text{AD}} = \sum_{m=1}^M \beta_m \log_2(1 + \gamma_{m,n}^{\text{AD}}), \forall n. \quad (8)$$

On the other hand, when decoding the backscattering signal, the DL signal can be regarded as perfectly removing from $\mathbf{y}_{m,n}^{\text{AP}}$ via SIC [30]. Thus, the received signal from the n -th BD at the AP can be expressed as

$$\bar{\mathbf{y}}_{m,n}^{\text{AP}} = \sqrt{\alpha_n P_m} h_{m,n}^{\text{f}} (\mathbf{v}_{m,n}^{\text{B}})^{\text{H}} \mathbf{h}_n^{\text{b}} s_m c_n + (\mathbf{v}_{m,n}^{\text{B}})^{\text{H}} \mathbf{z}_{\text{AP}}, \forall m, n. \quad (9)$$

According to (9), the signal-to-noise ratio (SNR) for the n -th BD can be expressed as

$$\gamma_{m,n}^{\text{BD}} = \frac{\alpha_n |h_{m,n}^{\text{f}}|^2 |(\mathbf{v}_{m,n}^{\text{B}})^{\text{H}} \mathbf{h}_n^{\text{b}}|^2 P_m}{\sigma_w^2}, \forall m, n. \quad (10)$$

The average throughput of the n -th BD can be obtained as the product of the corresponding achievable throughput and the its probability of successful channel access, which yields

$$R_n^{\text{BD}} = \Pr(n) \sum_{m=1}^M \beta_m r_{m,n}^{\text{BD}}, \forall n, \quad (11)$$

where $r_{m,n}^{\text{BD}} = \log_2(1 + \gamma_{m,n}^{\text{BD}})$ represents the achievable throughput of the n -th BD.

D. Problem Formulation

Our purpose is to find a performance-fair access scheme for multi-BD BackCom systems with the SA by optimizing the TAS factor and transmit power of the AD, the CAP and RC of each BD, as well as the receive beamforming vector, where the QoS requirements of the AD, and the EH demands of BDs are taken into account. Mathematically, the optimization problem can be formulated as

$$\begin{aligned} & \max_{\beta_m, q_n, P_m, \alpha_n, \mathbf{v}_{m,n}} \min_{\forall n} R_n^{\text{BD}} \\ \text{s.t. } & C_1 : \beta_m \in \{0, 1\}, \sum_{m=1}^M \beta_m = 1, \\ & C_2 : 0 < q_n < 1, \forall n, \\ & C_3 : R_n^{\text{AD}} \geq R_{\min}, \forall n, \\ & C_4 : \Phi_n(P_n^{\text{EH}}) \geq P_n^{\text{C}}, \forall n, \\ & C_5 : 0 < \alpha_n \leq 1, \forall n, \\ & C_6 : \sum_{m=1}^M \beta_m P_m \leq P_{\max}, \\ & C_7 : \|\mathbf{v}_{m,n}\|^2 = 1, \forall m, n, \end{aligned} \quad (12)$$

where R_n^{\min} denotes the minimum required throughput of the AD with the n -th accessed BD. P_n^{C} is the circuit power of the n -th BD. P_{\max} represents the maximum transmit power of the AD. It is worth detailing that C_1 can limit the selection factors for TAs, which means that only one TA can be selected for transmission. C_2 is used to limit the CAP of each BD. C_3 can ensure the QoS requirement of the AD, which means the achievable throughput should not be influenced whichever BD is accessed. C_4 guarantees that the harvested energy of

the n -th BD is sufficient to maintain its operation. C_5 and C_6 impose limitations on the RC of the n -th BD and the transmit power of the m -th TA of the AD, respectively. C_7 qualifies the receive beamforming vectors.

It should be noted that, we concentrate on exploring the random access for multiple devices in one time slot in this paper, which manifests a random access competition rather than being scheduled in advance (i.e., [33] and [34]) and is in contrast to the random access for multiple time slots (i.e., [26] and [29]). Beyond that, the fairness of the average throughput among different BDs is effectively guaranteed by assigning different CAPs, which can combat the unfairness caused by traditional tag selection.

III. ALGORITHM DESIGN

It is clear that problem (12) is intractable to be solved due to the non-convexity caused by the non-smooth objective function and the coupling of variables. In this section, we are going to design an effective algorithm for this problem. Specifically, the max-min form of the objective function is first removed by using a slack variable. Second, the resulting problem is decomposed into three sub-problems, and different algorithms are designed to solve them separately. Finally, according to the proposed BCD-based greedy method with MRC and SDP, the sub-optimal solution of problem (12) is obtained.

A. Problem Reformulation

It is hard to solve problem (12) due to the non-smooth objective function posed by the max-min form. To deal with this, a slack variable t is introduced, such that $\min_{\forall n} R_n^{\text{BD}} \geq t$. By doing so, the multi-objective problem can be transformed into a single-objective one, which can be equivalently expressed as

$$\begin{aligned} & \max_{\beta_m, q_n, P_m, \alpha_n, \mathbf{v}_{m,n}, t} t \\ & \text{s.t. } C_1 \sim C_7, \\ & C_8 : \Pr(n) \sum_{m=1}^M \beta_m r_{m,n}^{\text{BD}} \geq t, \forall n. \end{aligned} \quad (13)$$

Nonetheless, there are still many obstacles in solving problem (13), especially since there are strong coupled relationships of optimization variables among constraints, and both binary and continuous variables are involved. Regrettably, for such a non-convex problem, none of the existing methods can be directly used here to allow us to enjoy the hands-down benefits. This motivates us to design a BCD algorithm to solve it. Specifically, problem (13) is decomposed into three sub-problems, namely, the sub-problem for beamforming design, the sub-problem for power control and RC optimization, and the sub-problem for CAP determination.

B. The Sub-problem for Beamforming Design

With fixed β_m , P_m , q_n , and α_n , the sub-problem for beamforming design can be formulated as

$$\begin{aligned} & \max_{\mathbf{v}_{m,n}, t} t \\ & \text{s.t. } C_3, C_7, C_8. \end{aligned} \quad (14)$$

Algorithm 1: The Algorithm for Solving Problem (19)

Input: Fixed α_n , β_m , P_m , q_n .

Output: $\mathbf{v}_{m,n}^A$.

Data: Set the iteration index $i_{A1} = 1$, the tolerance ω_{th} , the maximum iteration number I_{A1} .

```

1 while  $|V_{m,n}^A(i_{A1} + 1) - V_{m,n}^A(i_{A1})| \geq \omega_{\text{th}} \parallel i_{A1} \leq I_{A1}$  do
2   | Solve problem (19) by using CVX to obtain
   |  $\mathbf{V}_{m,n}^A(i_{A1} + 1)$ .
3   |  $i_{A1} = i_{A1} + 1$ .
4 end
5 Update  $(\mathbf{V}_{m,n}^A)^* = \mathbf{V}_{m,n}^A(i_{A1})$ .
```

Let us first consider $\mathbf{v}_{m,n}^B$, which is only involving C_8 and is monotonically increasing with respect to the objective function. Thus, the MRC can be used to obtain the optimal $\mathbf{v}_{m,n}^B$, which can be given by

$$(\mathbf{v}_{m,n}^B)^* \triangleq \frac{\mathbf{h}_n^b}{\|\mathbf{h}_n^b\|}, \forall n. \quad (15)$$

Therefore, optimal t for problem (14) can be obtained as

$$t^* = \min_{\forall n} \Pr(n) \bar{r}_{m,n}^{\text{BD}}, \quad (16)$$

$$\text{where } \bar{r}_{m,n}^{\text{BD}} = \log_2 \left(1 + \frac{\alpha_n |\mathbf{h}_{m,n}^f|^2 \|\mathbf{h}_n^b\|^2 P_m}{\sigma_w^2} \right).$$

However, $\mathbf{v}_{m,n}^A$ still remains unsolved. To deal with it, an optimization problem involved $\mathbf{v}_{m,n}^A$ is decomposed, which can be rewritten as

$$\begin{aligned} & \max_{\mathbf{v}_{m,n}^A} t^* \\ & \text{s.t. } C_3, C_7. \end{aligned} \quad (17)$$

Distressingly, problem (17) is still non-convex due to the non-linearity of beamforming vector in C_3 . To make it tractable, a new variable is applied, such as $\mathbf{V}_{m,n}^A = \mathbf{v}_{m,n}^A (\mathbf{v}_{m,n}^A)^H$, problem (17) can be equivalently rewritten by

$$\begin{aligned} & \max_{\mathbf{V}_{m,n}^A} t^* \\ & \text{s.t. } C_{3-1}^{\text{BF}} : \left(2^{\bar{R}^{\text{min}}} - 1 \right) \left(\text{Tr}(\mathbf{H}_n^b \mathbf{V}_{m,n}^A) \alpha_n |\mathbf{h}_{m,n}^f|^2 P_m + \sigma_w^2 \right) \\ & \leq \text{Tr}(\mathbf{H}_m^d \mathbf{V}_{m,n}^A) P_m, \forall n, \\ & C_{7-1}^{\text{BF}} : \text{Tr}(\mathbf{V}_{m,n}^A) = 1, \forall n, \\ & C_9^{\text{BF}} : \text{Rank}(\mathbf{V}_{m,n}^A) = 1, \forall n, \\ & C_{10}^{\text{BF}} : \mathbf{V}_{m,n}^A \succeq 0, \forall n, \end{aligned} \quad (18)$$

where $\mathbf{H}_m^d = \mathbf{h}_m^d (\mathbf{h}_m^d)^H$ and $\mathbf{H}_n^b = \mathbf{h}_n^b (\mathbf{h}_n^b)^H$.

Yet despite that, problem (18) is still challenging to solve, since the rank-one constraint C_9^{BF} is non-convex. To deal with this, we first dropped C_9^{BF} to obtain a standard SDP problem [35], i.e.,

$$\begin{aligned} & \max_{\mathbf{V}_{m,n}^A} t^* \\ & \text{s.t. } C_{3-1}^{\text{BF}}, C_{7-1}^{\text{BF}}, C_{10}^{\text{BF}}. \end{aligned} \quad (19)$$

Note that problem (19) is a convex optimization problem and its solution can be obtained via CVX [36]. The proposed algorithm for solving (19) is summarized in **Algorithm 1**.

For proceeding, we have the following theorem.

Theorem 1: The optimal solution $((\mathbf{V}_{m,n}^A)^*)$ to problem (19)

$$P_m^* = P_{\max} > \max \left\{ \frac{\Phi_n^{-1}(P_n^C)}{|h_{m,n}^f|^2}, \frac{(2^{R_{\min}} - 1) \sigma_w^2}{\text{Tr}(\mathbf{H}_m^d \mathbf{V}_{m,n}^A)} \right\} \triangleq P_{m,n}^{\min}, \forall n, \quad (21a)$$

$$\alpha_n^* = \left[\min \left\{ \underbrace{\frac{\text{Tr}(\mathbf{H}_m^d \mathbf{V}_{m,n}^A) P_{\max} - (2^{R_{\min}} - 1) \sigma_w^2}{(2^{R_{\min}} - 1) \text{Tr}(\mathbf{H}_n^b \mathbf{V}_{m,n}^A) |h_{m,n}^f|^2 P_{\max}}}_{\alpha_n^{\text{AD}}}, \underbrace{1 - \frac{\Phi_n^{-1}(P_n^C)}{P_{\max} |h_{m,n}^f|^2}}_{\alpha_n^{\text{EH}}} \right\} \right]^+, \forall n. \quad (21b)$$

$$\bar{t}_n^* = \begin{cases} \Pr(n) \log_2 \left(1 + \frac{\text{Tr}(\mathbf{H}_m^d \mathbf{V}_{m,n}^A) P_{\max} - (2^{R_{\min}} - 1) \sigma_w^2}{(2^{R_{\min}} - 1) \text{Tr}(\mathbf{H}_n^b \mathbf{V}_{m,n}^A) \sigma_w^2} \|\mathbf{h}_n^b\|^2 \right), \alpha_n^{\text{AD}} < \alpha_n^{\text{EH}}, \forall n, \\ \Pr(n) \log_2 \left(1 + \frac{|h_{m,n}^f|^2 \|\mathbf{h}_n^b\|^2 P_{\max} - \|\mathbf{h}_n^b\|^2 \Phi_n^{-1}(P_n^C)}{\sigma_w^2} \right), \alpha_n^{\text{AD}} \geq \alpha_n^{\text{EH}}, \forall n. \end{cases} \quad (22)$$

satisfies $\text{Rank}((\mathbf{V}_{m,n}^A)^*) = 1$.

Proof: Please see Appendix A.

Remark 1: From Theorem 1, it follows that the optimal solution $(\mathbf{V}_{m,n}^A)^*$ to problem (19) satisfies the rank-one constraint naturally, thus it is also the globally optimal solution to problem (18). The eigenvalue decomposition of $(\mathbf{V}_{m,n}^A)^*$ is denoted as $(\mathbf{V}_{m,n}^A)^* = \mathbf{Q}\mathbf{\Lambda}\mathbf{Q}^H$. Denote the unique non-zero eigenvalue of $(\mathbf{V}_{m,n}^A)^*$ by $\lambda_{m,n}^*$, and the corresponding eigenvector by $\mathbf{u}_{m,n}^*$. The optimal solution to problem (14) can be obtained as $\sqrt{\lambda_{m,n}^*} \mathbf{u}_{m,n}^*$.

C. The Sub-problem for Power Control and RC Optimization

With fixed q_n , β_m , and $\mathbf{v}_{m,n}$, the sub-problem for power control and RC optimization can be formulated as

$$\begin{aligned} & \max_{P_m, \alpha_n, \bar{t}} \bar{t} \\ & \text{s.t. } C_{3-1}^{\text{BF}}, C_5, \\ & C_{4-1}^{\text{PR}} : (1 - \alpha_n) P_m |h_{m,n}^f|^2 \geq \Phi_n^{-1}(P_n^C), \forall n, \quad (20) \\ & C_{6-1}^{\text{PR}} : P_m \leq P_{\max}, \\ & C_{8-1}^{\text{PR}} : \Pr(n) \bar{r}_{m,n}^{\text{BD}} \geq \bar{t}, \forall n, \end{aligned}$$

where \bar{t} is the slack variable, $\Phi_n^{-1}(x) = \lceil \frac{b_n - \ln A_n}{a_n} \rceil^+$ is the inverse function of Φ_n , $A_n = \frac{1 + \exp(-a_n P_n^{\text{SE}} + b_n)}{B_n x + 1}$, and $B_n = \frac{\exp(-a_n P_n^{\text{SE}} + b_n)}{P_n^{\text{SA}}}$.

It can be seen that problem (20) is non-convex due to the tightly coupled variables in constraints C_{3-1}^{BF} , C_{4-1}^{PR} , and C_{8-1}^{PR} . To solve this problem, we propose the following theorem.

Theorem 2: With fixed q_n , β_m , and $\mathbf{v}_{m,n}$, the optimal P_m^* and α_n^* can be derived as (21a) and (21b), respectively.

Proof: Please see Appendix B.

Remark 2: The feasible region for P_{\max} is expressed as (21a), which can guide us in setting the maximum transmit power of the AD, whose value should be at least higher than this lower bound for QoS support. From (21b), it can be extrapolated that α_n^{AD} decreases with the increasing $|h_{m,n}^f|^2$ and/or the decreasing $\text{Tr}(\mathbf{H}_m^d \mathbf{V}_{m,n}^A)$. The reason is that the enhanced backscattering link and/or the decreased DL incur more interference for the AD, thus the RC of the accessed BD has to reduce to satisfy the QoS of the AD. Besides, α_n^{AD}

is also shrinking with the increased R_{\min} since when R_{\min} is improved, the corresponding SINR for the AD also needs to maintain the consistent trend, which reduces the tolerance for interference signal (i.e., backscattering signal). On the other hand, α_n^{EH} decreases as P_{\max} and/or $|h_{m,n}^f|^2$ become smaller. This is due to the fact that the decreasing P_{\max} and/or $|h_{m,n}^f|^2$ make the harvested energy of each BD reduce, and the ratio of energy allocated to compensate for the circuit increases accordingly. In summary, the scale will be biased towards α_n^{AD} when the channel gain of the backscattering link is stronger, or when a higher rate for the AD is desired. Conversely, there is a preference for α_n^{EH} .

Then, the optimal \bar{t} for problem (20) can be obtained by substituting (21a) and (21b) into problem (20), which can be expressed as $\bar{t}^* = \min t_n^*$, where t_n^* is expressed as (22).

D. The Sub-problem for CAP Determination

Let us consider q_n in this subsection with the fixed β_m , α_n , P_m , and $\mathbf{v}_{m,n}$. The sub-problem for CAP determination can be expressed as

$$\begin{aligned} & \max_{q_n, \hat{t}} \hat{t} \\ & \text{s.t. } C_2, \\ & C_{8-1}^{\text{CD}} : \Pr(n) \bar{r}_{m,n}^{\text{BD}} \geq \hat{t}, \forall n. \end{aligned} \quad (23)$$

where \hat{t} is the slack variable.

However, multivariate decision is an obstacle to solving problem (23). To make it treatable, it can be equivalently transformed into

$$\begin{aligned} & \max_{q_n, \hat{t}} \hat{t} \\ & \text{s.t. } C_2, \\ & C_{8-2}^{\text{CD}} : \ln q_n + \sum_{j=1, j \neq n}^N \ln(1 - q_j) + \ln \bar{r}_{m,n}^{\text{BD}} \geq \ln \hat{t}, \forall n. \end{aligned} \quad (24)$$

Regrettably, problem (24) is still challenging due to the non-linearity of the constraints. To deal with it, we make the

Algorithm 2: The Algorithm for Solving Problem (25)**Input:** Fixed $\beta_m, \alpha_n, P_m, \mathbf{v}_{m,n}$.**Output:** q_n .**Data:** Set the iteration index $i_{A2} = 1$, the tolerance ϕ_{th} , the maximum iteration number I_{A2} .

- 1 **while** $|\bar{t}''(i_{A2} + 1) - \bar{t}''(i_{A2})| \geq \phi_{th} \parallel i_{A2} \leq I_{A2}$ **do**
- 2 Given/Update $\hat{q}_j(i_{A2})$, solve problem (25) to obtain $\bar{q}_n(i_{A2}), \hat{q}_n(i_{A2})$, and $\bar{t}''(i_{A2})$.
- 3 $i_{A2} = i_{A2} + 1$.
- 4 **end**
- 5 Calculate $q_n^* = \exp(\bar{q}_n(i_{A2}))$ and $(t'')^* = \exp(\bar{t}''(i_{A2}))$.

Algorithm 3: The BCD-Based Greedy Algorithm**Input:** $K, M, N, h_{m,n}^f, \mathbf{h}_m^d, \mathbf{h}_n^b, \sigma_w^2, \sigma_n^2, R_{min}, P_n^C, P_{max}, P_n^{SA}, P_n^{SE}, a_n, b_n$.**Output:** $P_m, \alpha_n, \beta_m, q_n, \mathbf{v}_{m,n}$.**Data:** Set the initial point $t_0 = 0$, the iteration index $i_{A3} = 1$, the tolerance ε_{th} , and the maximum iteration number I_{A3} .

- 1 **for** $m = 1 : M$ **do**
- 2 Set $\beta_m = 1$.
- 3 **do**
- 4 **Algorithm 1:** Given $\alpha_n(i_{A3}), P_m(i_{A3})$, and $q_n(i_{A3})$, solve problems (14) and (19) to obtain $\mathbf{v}_{m,n}(i_{A3}+1)$ and $t(i_{A3}+1)$
- 5 **Closed form:** Given $\mathbf{v}_{m,n}(i_{A3}+1)$ and $q_n(i_{A3})$, solve problem (20) to obtain $P_m(i_{A3}+1), \alpha_n(i_{A3}+1)$ and $\bar{t}(i_{A3}+1)$.
- 6 **Algorithm 2:** Given $P_m(i_{A3}+1), \mathbf{v}_{m,n}(i_{A3}+1)$ and $\alpha_n(i_{A3}+1)$, solve problem (25) to obtain $q_n(i_{A3} + 1)$ and $\hat{t}(i_{A3}+1)$.
- 7 $i_{A3} = i_{A3} + 1$.
- 8 **while** $|t(i_{A3}) - \bar{t}(i_{A3})| \leq \varepsilon_{th} \& \& |t(i_{A3}) - \hat{t}(i_{A3})| \leq \varepsilon_{th} \parallel i_{A3} > I_{A3}$;
- 9 Update $t_{conv}(m) = t(i_{A3})$.
- 10 **if** $t_{conv}(m) - t_0 \leq 0$ **then**
- 11 | Set $\beta_m = 0$.
- 12 **else**
- 13 | Update $t_0 = t_{conv}(m)$.
- 14 **end**
- 15 **end**

following transformation, i.e.,

$$\begin{aligned}
 & \max_{\bar{q}_n, \hat{q}_n, \tilde{t}} \tilde{t} \\
 & \text{s.t. } C_{2-1}^{CD} : \bar{q}_n < 0, \hat{q}_n < 0, \forall n, \\
 & C_{8-3}^{CD} : \bar{q}_n + \sum_{j=1, j \neq n}^N \hat{q}_j \geq \tilde{t} - \ln \bar{r}_{m,n}^{BD}, \forall n, \\
 & C_{11}^{CD} : \exp(\bar{q}_n) + \exp(\hat{q}_n) \leq 1, \forall n,
 \end{aligned} \tag{25}$$

where $\bar{q}_n = \ln q_n, \hat{q}_n = \ln(1 - q_n)$, and $\tilde{t} = \ln \hat{t}$.

So far, problem (25) is a standard convex problem, which can be solved efficiently using the numerical evaluation [36]. The details of this algorithm are given by **Algorithm 2**.

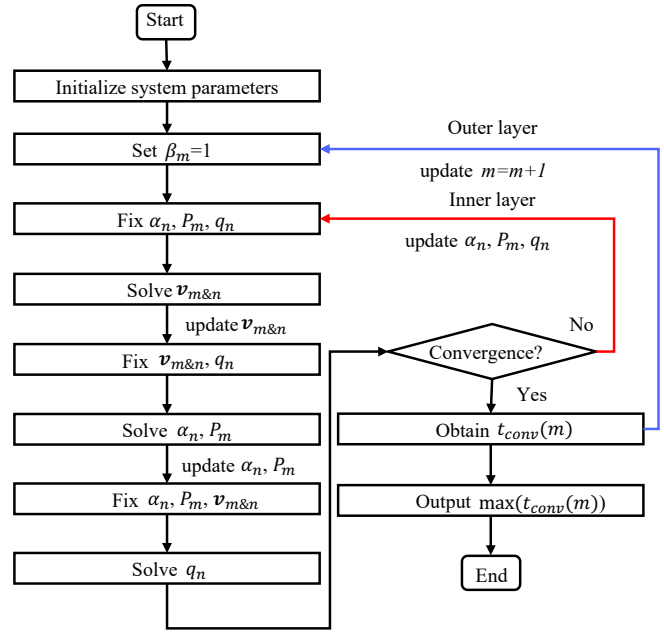


Fig. 3. The flowchart of Algorithm 3.

E. The Greedy Algorithm for TAS

In the previous subsections, the beamforming vectors, the transmit power of the AD, and the RC and CAP of each BD have been obtained separately. How to select the optimal TA for transmission still remains unsolved. In what follows, we will tackle this issue. It is noted that the problem of TAS is a 0-1 non-linear problem, which is NP-complete. This motivates us to design a greedy algorithm to obtain the optimal TAS factor, which is detailed in **Algorithm 3**, where $t_{conv}(m)$ denotes the convergence point of proposed algorithm under the m -th TA. Specifically, this algorithm adopts an alternating optimization method to iteratively optimize the sub-problems for beamforming design, power control and RC optimization, and CAP determination in the inner-layer. The outer-layer then obtains the TAS factor through a search process. For the sake of intuition, the flowchart of Algorithm 3 is further provided, as shown in Fig. 3.

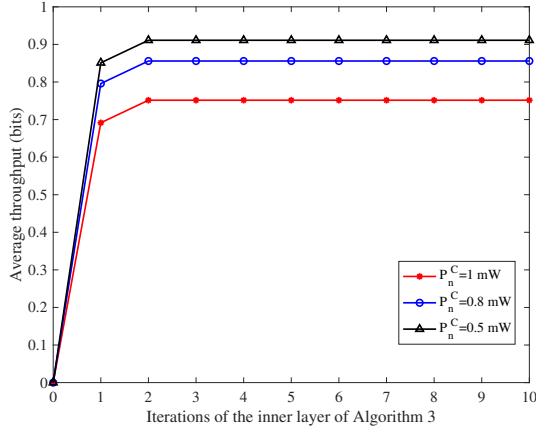
F. Convergence and Complexity Analysis

In this subsection, we analyze the convergence and complexity of the proposed algorithm. First, we provide an analysis of the convergence of **Algorithm 3**. Since the greedy algorithm does not affect the convergence of **Algorithm 3**, we mainly focus on the convergence of the inner-layer BCD-based algorithm. For completeness, we provide the following theorem.

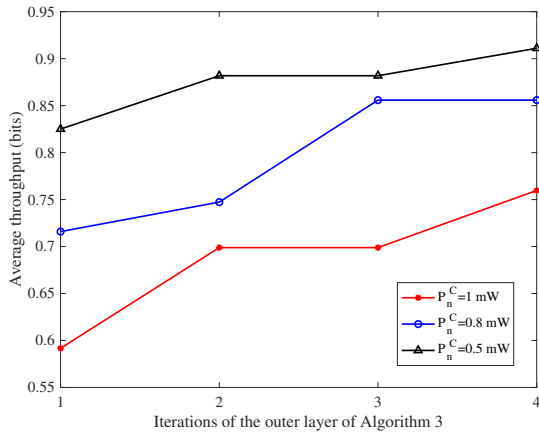
Theorem 3: The convergence of **Algorithm 3** is guaranteed.

Proof: Please see Appendix C.

Next, the computational complexity for **Algorithm 3** is evaluated. For the sub-problem for beamforming design, the complexity includes solving the beamforming vectors of the passive and active signals with MRC and **Algorithm 1**, respectively. Specifically, given the number of BDs, it only costs $\mathcal{O}(N)$ operation for solving the beamforming vector



(a) The convergence of the inner layer of Algorithm 3.



(b) The greedy process of the outer layer of Algorithm 3.

Fig. 4. The effectiveness of Algorithm 3.

of passive signal via MRC. For **Algorithm 1**, given the number of constraints, interior point method with a matrix variable $\mathbf{V}_{m,n}^A$ of size $K \times K$ will take $\mathcal{O}(\sqrt{NK} \ln(1/\omega_{\text{th}}))$ iterations, with each iteration requiring $\mathcal{O}(N^3 K^6)$ arithmetic operations for the worst case, where ω_{th} denotes the precision of the interior point algorithm [37]. Therefore, the computational complexity for the beamforming design is $\mathcal{O}_{\text{BF}} = \mathcal{O}(N^{3.5} K^{6.5} \ln(1/\omega_{\text{th}}) + N)$. For the sub-problem for power control and RC optimization, solving the transmit power and RC of each BD only requires $\mathcal{O}(1)$ and $\mathcal{O}(N)$ operations, respectively. Thus, we can obtain the computational complexity for this sub-problem is $\mathcal{O}_{\text{PR}} = \mathcal{O}(N)$, ignoring the low-complexity item. For the sub-problem for CAP determination, the computational complexity is $\mathcal{O}_{\text{CD}} = \mathcal{O}(N^{3.5} \ln(1/\omega_{\text{th}}))$ for operating **Algorithm 2**. Thus, defining I_{A3} as the maximum alternating iteration number, the computational complexity of the inner layer of **Algorithm 3** can be obtained as $\mathcal{O}_{\text{Inner}} = \mathcal{O}(I_{A3}(\mathcal{O}_{\text{BF}} + \mathcal{O}_{\text{PR}} + \mathcal{O}_{\text{CD}}))$. Besides, the computational complexity of the outer layer of **Algorithm 3** is $\mathcal{O}(M)$. Overall, the total computational complexity of **Algorithm 3** can be calculated as $\mathcal{O}(M\mathcal{O}_{\text{Inner}})$.

TABLE III
 R_λ WITH DIFFERENT K

BD	1	2	3	4
$K = 2$	7.85e-17	-2.16e-17	-3.93e-27	-1.18e-16
$K = 4$	-8.20e-18	1.47e-17	-3.53e-17	2.02e-16

IV. SIMULATION RESULTS

In this section, simulation results are provided to evaluate the performance of the proposed algorithm. The system parameters are first provided. Then, we evaluate the proposed algorithm in the following three aspects, namely algorithm effectiveness, algorithm comparison, and algorithm fairness.

A. Simulation Setup

We assume that there are one AD with 4 transmit antennas, 4 single-antenna BDs, and one AP with 4 antennas in the considered system. The coordinates of the AD and the AP are (0, 0) m and (6, 0) m, respectively. All the tags are randomly distributed in a circle with the center's coordinate being (3, 3) m and $r = 2$ m is the radius of the circle. The distance-dependent pass loss is modeled by $P_L = d^{-\mu}$, in which d denotes the Euclidean distance in meters and $\mu = 2.2$ is the path loss exponent. Besides, Rician fading is applied as small-scale fading for all channels, where the Rician factor is 2.8 dB. Other parameters include $P_{\text{max}} = 1$ W, $R_{\text{min}} = 1$ bits, $P_n^C = 1$ mW, $a_n = 274$, $b_n = 0.29$, $P_n^{\text{SE}} = 0.064$ mW, $P_n^{\text{SA}} = 4.927$ mW [32], and $\sigma_n^2 = \sigma_w^2 = 10^{-8}$ W. The iteration termination thresholds ω_{th} , ϕ_{th} , and ε_{th} are both set as 10^{-3} . Besides, the maximum iteration numbers I_{A1} , I_{A2} , and I_{A3} are both set as 10^3 . Finally, all simulation results are based on the CVX package [38].

B. The Algorithm Effectiveness

In this subsection, the effectiveness of the proposed algorithm is provided, as shown in Fig. 4 for different values of P_n^C . As shown in Fig. 4(a), the inner layer of the proposed algorithm converges within three iterations, indicating stable performance. The optimal TAS can also be quickly obtained through greedy search, as shown in Fig. 4(b). Notably, the average throughput increases with decreasing P_n^C . This is due to the need for additional harvested energy to satisfy the higher circuit power consumption, which decreases the backscattering power. This finding highlights the trade-off between the circuit power consumption and the backscattering power.

Additionally, we investigate the rank of the obtained beamforming matrix $(\mathbf{V}_{m,n}^A)^*$ using the method presented in [39]. Table III shows the values of the ratio R_λ between the second largest eigenvalue and the largest eigenvalue of $(\mathbf{V}_{m,n}^A)^*$ for different numbers of receive antennas (K). The results show that the minimum value of R_λ is consistently close to zero, indicating that the solutions obtained by the proposed algorithm are always rank-one, regardless of the value of K . This finding provides further support for the proof presented in Appendix A.

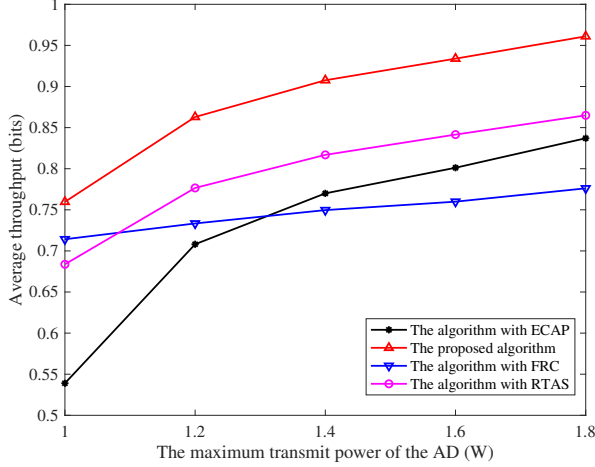


Fig. 5. The average throughput versus the transmit power of the AD.

C. The Algorithm Comparison

In this subsection, the comparison of the related algorithms is provided. To better demonstrate this property, some benchmark algorithms are defined and compared, such as

- **The algorithm with equal CAP (ECAP):** In this algorithm, each BD is endowed with the same CAP. This algorithm can be obtained from the proposed algorithm by setting the CAP of each BD as $1/N$, which can reduce the computation complexity for solving CAP.
- **The algorithm with fixed RC (FRC):** In this algorithm, the RC of each BD is set to a constant and no longer changes dynamically. This algorithm can be obtained from the proposed algorithm by setting the RC of each BD to a constant.
- **The algorithm with random TAS (RTAS):** Different from the proposed algorithm, each TA is selected randomly under this algorithm. This algorithm can be obtained from the proposed algorithm by replacing the greedy algorithm with a random approach, which can reduce the computation complexity for solving TAS.
- **The algorithm with TDMA:** In this algorithm, TDMA is adopted (i.e., [11]), in which multiple BDs take turns to backscatter their own signal. This results in a new optimization problem, which is detailed in Appendix D.
- **The algorithm with transmission collision (TC):** All BDs are accessed simultaneously in this algorithm (i.e., [30]), which poses strong MI among BDs and is different from the above collision-free algorithms. This also results in a new optimization problem, which is detailed in Appendix D.

1) **Comparison under same access protocol:** First, the performance of the proposed algorithm is verified by comparing with the benchmarks under the same access protocol, i.e., the SA.

Fig. 5 presents the average throughput versus the maximum transmit power of the AD (P_{\max}). As shown in the figure, the average throughput of all algorithms increases as P_{\max} increases. This can be attributed to the monotonic increase of the average throughput of the BD (i.e., R_n^{BD} in (11))

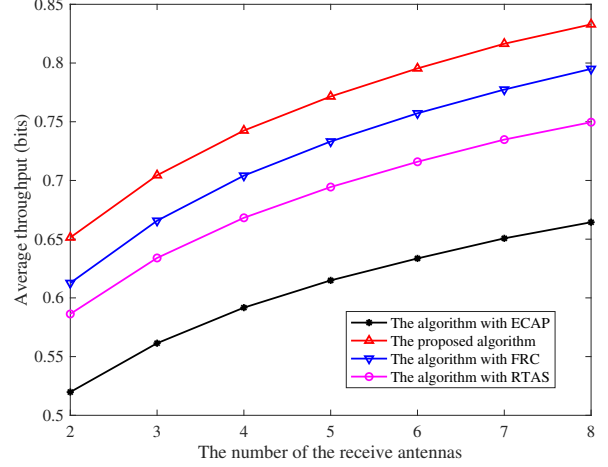


Fig. 6. The average throughput versus the number of receive antennas.

with respect to the transmit power. Moreover, the proposed algorithm exhibits a higher average throughput than the other algorithms. This is because the algorithms with FRC and ECAP cannot be adjusted dynamically, which results in slight mismatches in resource allocation and is more apparent when P_{\max} is higher. Furthermore, the algorithm with RTAS has inherent uncertainty and may not consistently ensure high-quality transmission.

Fig. 6 reveals the average throughput versus the number of receive antennas of the AP (K). It is observed that the average throughput of all algorithms increases as K increases. This can be explained by the fact that the increasing K makes the beamforming gains increase and thus the SNR of the BD increase. Additionally, the algorithm with ECAP exhibits the lowest average throughput. This is because the algorithm with ECAP places too much emphasis on access fairness (i.e., q_n) and ignores channel differences between BDs, especially, more receive antennas are involved, which enlarge the performance gap with the proposed algorithm. In contrast to the algorithm with FRC, the proposed algorithm can adjust the resource control of each BD to avoid the over-harvesting energy, thereby improving the backscattered signal power.

Fig. 7 presents the average throughput versus the number of BDs (N). As can be seen from the figure, the average throughput of all algorithms decreases gradually with increasing N . This can be attributed to the decrease in the CAP of each BD (q_n) as N increases, leading to a lower successful CAP (i.e., $\Pr(n)$) and a reduced effective average throughput. Besides, as N gets larger, the gap between different algorithms gradually shrinks. This gives us enlightenment, that is, when the number of BDs involved is large, the proposed algorithm can be approximated by these benchmark algorithms, which can reduce the computational complexity used to optimize CAP, RC, and/or TAS.

Fig. 8 shows the average throughput versus the noise power at the AP (σ_w^2). As expected, the average throughput of all algorithms decreases gradually with increasing σ_w^2 . This is because the higher noise power leads to a decrease in the

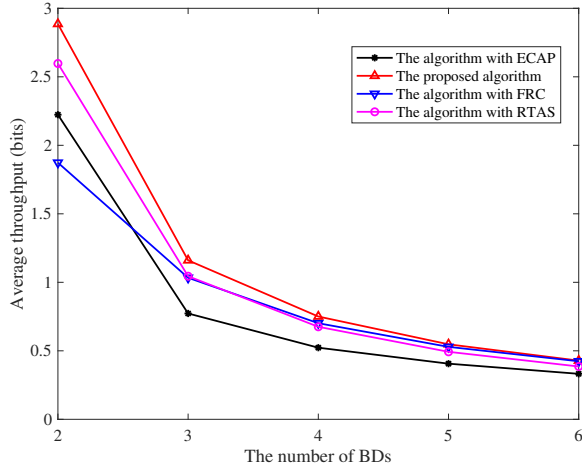


Fig. 7. The average throughput versus the number of BDs.

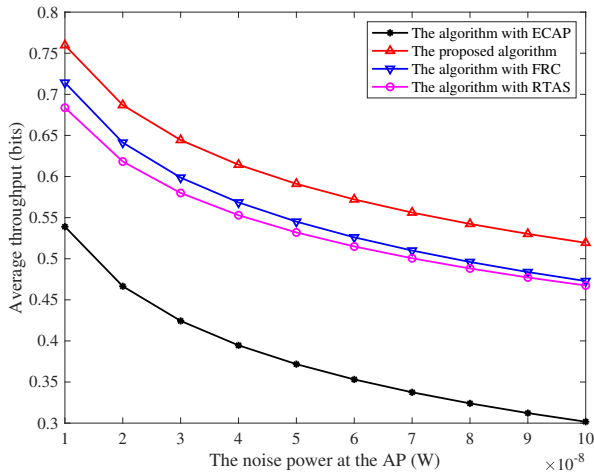


Fig. 8. The average throughput versus the noise power of the AP.

SNR of both active and passive communications, which is evident from (7) and (10), resulting in a reduced achievable throughput. Additionally, as σ_w^2 increases, the downward trend of the average throughput of all algorithms slows down, due to the non-linear nature of the logarithmic function in R_n^{BD} . Overall, this observation highlights the delicate balance between the background noise and the average throughput.

2) **Comparison under different access protocol:** In this part, we are going to evaluate the performance of the proposed algorithm from the perspective of different access protocols. To ensure impartiality, we compare the performance of the proposed algorithm to that of other access protocol-based algorithms via the achievable throughput of the BackCom system in one transmission time slot, rather than relying solely on average throughput metrics.

Fig. 9 demonstrates the practical backscattering throughput versus the transmit power of the AD (P_{\max}). It can be seen from the figure that the performance of the algorithm with TC is significantly lower than that of the other algorithms. This is due to the strong MI caused by the parallel transmission of multiple BDs, which makes the SINR of each BD relatively

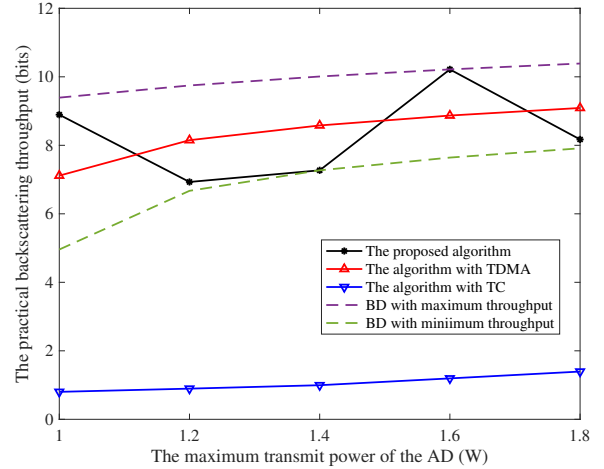


Fig. 9. The practical backscattering throughput versus the transmit power of the AD.

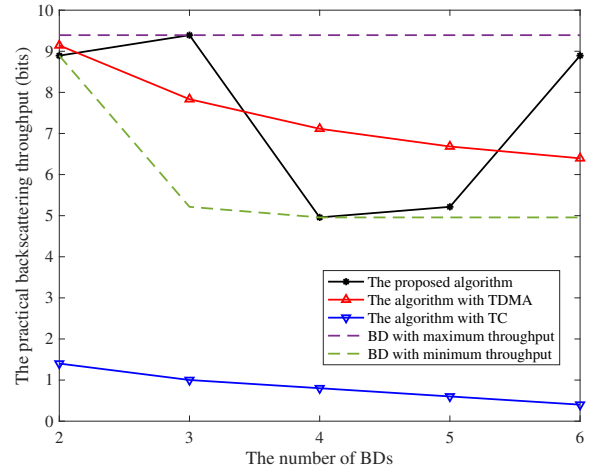


Fig. 10. The practical backscattering throughput versus the number of BDs.

low and thus results in poor performance. On the other hand, the algorithm with TDMA shows strong stability, with its performance gradually increasing with the increase of P_{\max} . However, the performance of the proposed algorithm exhibits fluctuations due to the random access of BDs with different channel states, even though the throughput of each individual BD (i.e., the BDs with maximum and minimum throughput) also increases with the increase of P_{\max} .

Fig. 10 presents the practical backscattering throughput versus the number of BDs (N). As shown in the figure, as N increases, the achievable throughput of the algorithms with TDMA and TC decreases gradually. For the algorithm with TC, the increasing N exacerbates the MI between BDs, resulting in extremely low performance; for the algorithm with TDMA, the transmission time of each BD is compressed to satisfy their QoS requirements, leading to a decrease in the system performance. Besides, the performance of the proposed algorithm fluctuates within a performance range, the upper and lower bounds of which depend on the channel condition of the BDs being accessed. The reason for this lies in the fact that

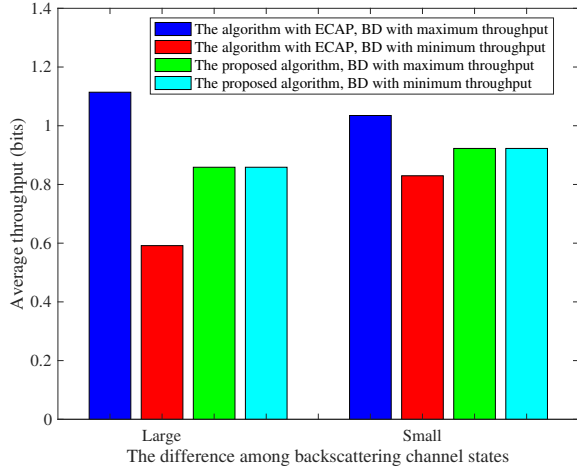


Fig. 11. The average throughput versus the different backscattering channel state.

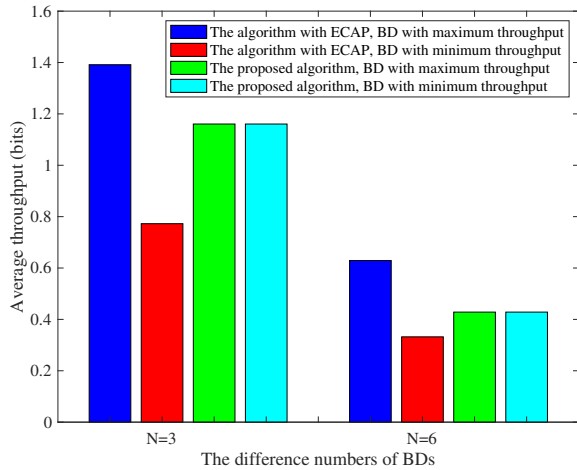


Fig. 12. The average throughput versus the different number of BDs.

the proposed algorithm randomly selects a BD from multiple BDs for access within a system time slot, which is different from other algorithms.

Overall, the proposed algorithm, which adopts a collision-free transmission scheme, is beneficial for the transmission of the BackCom system compared to the algorithm with TC. On the other hand, the algorithm with TDMA also provides collision-free transmission. However, it requires central control for implementation, although its performance stability is better than that of the proposed algorithm. However, the proposed algorithm is implemented based on a decentralized decision, and it has lower overhead compared to the TDMA architecture.

D. The algorithm Fairness

In this subsection, the performance of the proposed algorithm is compared to that of the algorithm with ECAP to evaluate fairness from the perspectives of the backscattering channel states and the number of BDs, respectively.

Fig. 11 presents the average throughput versus the difference backscattering channel states ($h_{m,n}^f h_n^b$). As can be seen,

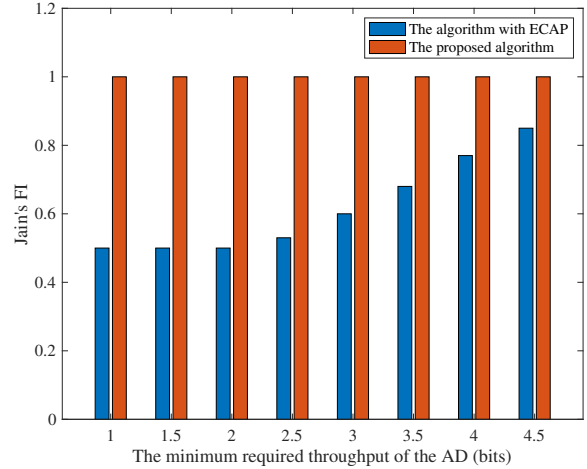


Fig. 13. The Jain's FI versus the minimum throughput of the AD.

when the difference between $h_{m,n}^f h_n^b$ for different BDs is small, the gap between the maximum and minimum average throughput of both algorithms is small, and even the gap of the proposed algorithm is close to zero. When it becomes large, the gap of the algorithm with ECAP increases, the gap between the maximum and minimum average throughput for the proposed algorithm remains relatively small. This is because the algorithm with ECAP disregards the differences in channels between different users, resulting in mismatched resources. However, the proposed algorithm places greater emphasis on balancing performance, which is a distinguishing feature between them.

Fig. 12 shows the average throughput versus the number of BDs (N). As can be seen, the average throughput is decreasing as N increases, consistent with Fig. 7. Besides, it can also be seen that regardless of N , the average throughput of each BD is almost equal for the proposed algorithm, while there is a significant difference in the average throughput between BDs under the algorithm with ECAP. This is because the proposed algorithm adopts a max-min form that can achieve absolute fairness in resource allocation.

Combining the above two figures, it can be asserted that the proposed algorithm is better in guaranteeing the transmission fairness regardless of channel differences and number of BDs, which is in contrast to the algorithm with ECAP.

Furthermore, in order to better measure the fairness of these two algorithm, Jain's fairness index (FI) is applied [40], namely $FI = (\sum_{n=1}^N R_n^{BD})^2 / (N \sum_{n=1}^N (R_n^{BD})^2)$. Specifically, Fig. 13 depicts the Jain's FI versus the minimum required throughput of the AD (R_{\min}). It can be seen that as R_{\min} increases, the FI of the algorithm with ECAP first keeps constant and then gradually increases. This can be explained by the increase in R_{\min} results in a corresponding increase in the SINR of the AD, thereby reducing the backscattering signal of the accessed BD, especially, the most immediate effect is that RC is limited by α_n^{AD} in (21b). That is to say, the performance gap with the BD with maximum and minimum throughput becomes smaller, which improves the fairness of

$$\begin{aligned} \mathcal{L}(t^*, \mathbf{V}_{m,n}^A, \chi_{m,n}, \varepsilon_{m,n}, \boldsymbol{\Omega}_{m,n}) &= t^* + \sum_{n=1}^N \chi_{m,n} \left\{ \text{Tr}(\mathbf{H}_m^d \mathbf{V}_{m,n}^A) P_m - (2^{R_{\min}} - 1) (\text{Tr}(\mathbf{H}_n^b \mathbf{V}_{m,n}^A) \alpha_n |h_{m,n}^f|^2 P_m + \sigma_w^2) \right\} \\ &+ \sum_{n=1}^N \varepsilon_{m,n} (1 - \text{Tr}(\mathbf{V}_{m,n}^A)) + \sum_{n=1}^N \text{Tr}(\mathbf{V}_{m,n}^A \boldsymbol{\Omega}_{m,n}) = t^* + \sum_{n=1}^N \text{Tr}(\mathbf{V}_{m,n}^A \mathbf{X}_{m,n}) - \sum_{n=1}^N \chi_{m,n} (2^{R_{\min}} - 1) \sigma_w^2 + \sum_{n=1}^N \varepsilon_{m,n}. \end{aligned} \quad (26)$$

$$P_m \geq \max \left\{ \frac{\Phi_n^{-1}(P_n^C)}{(1 - \alpha_n) |h_{m,n}^f|^2}, \frac{(2^{R_{\min}} - 1) \sigma_w^2}{\text{Tr}(\mathbf{H}_m^d \mathbf{V}_{m,n}^A) - (2^{R_{\min}} - 1) \text{Tr}(\mathbf{H}_n^b \mathbf{V}_{m,n}^A) \alpha_n |h_{m,n}^f|^2} \right\}. \quad (31)$$

this algorithm. Besides, the FI of the proposed algorithm is always close to 1, which indicates absolute fairness can be obtained. From this figure, we can conclude that the ECAP algorithm can be used to approximate the proposed algorithm when a higher R_{\min} is required, which can further reduce the computational complexity used to optimize CAP (i.e., q_n).

V. CONCLUSIONS

This paper investigates and analyzes the hybrid active-passive multiple-access BackCom system, where the SA-based protocol is introduced to overcome the high overhead problem of traditional multi-access protocols in dealing with massive devices, and an optimization problem for rate fairness is formulated. Then, we transform the objective function with the max-min form into an equivalent linear one by using a slack variable, and decompose the resulting problem into three sub-problems. Next, a BCD-based algorithm with MRC, SDP, and variable substitution is proposed to obtain the sub-optimal solutions. Simulation results demonstrate that the proposed algorithms outperform benchmark algorithms in terms of transmission performance and fairness.

APPENDIX A PROOF OF THEOREM 1

The Lagrangian function of the problem (19) is expressed as (26), where $\chi_{m,n}$ and $\varepsilon_{m,n}$ denote the dual variables associated with C_{3-1}^{BF} , C_{7-1}^{BF} , $\boldsymbol{\Omega}_{m,n}$ is the dual matrix associated with the positive semi-definite (PSD) constraint C_{10}^{BF} , and $\mathbf{X}_{m,n}$ is expressed as

$$\begin{aligned} \mathbf{X}_{m,n} &= \chi_{m,n} \left\{ \mathbf{H}_m^d P_m - (2^{R_{\min}} - 1) \mathbf{H}_n^b \alpha_n |h_{m,n}^f|^2 P_m \right\} \\ &- \varepsilon_{m,n} + \boldsymbol{\Omega}_{m,n}. \end{aligned} \quad (27)$$

Denoting $(\mathbf{V}_{m,n}^A)^*$, $\chi_{m,n}^*$, $\varepsilon_{m,n}^*$, and $\boldsymbol{\Omega}_{m,n}^*$ as the optimal original and dual variables, the Karush-Kuhn-Tucker (KKT) condition should be satisfied as follows

$$\nabla_{\mathbf{V}_{m,n}^A} \mathcal{L}((\mathbf{V}_{m,n}^A)^*, \chi_{m,n}^*, \varepsilon_{m,n}^*, \boldsymbol{\Omega}_{m,n}^*) = \mathbf{X}_{m,n}^* = \mathbf{0}, \quad (28)$$

and

$$(\mathbf{V}_{m,n}^A)^* \boldsymbol{\Omega}_{m,n}^* = \mathbf{0}, \quad (29)$$

where $\mathbf{X}_{m,n}^* = \boldsymbol{\Omega}_{m,n}^* - \varepsilon_{m,n}^* + \chi_{m,n}^* \mathbf{H}_m^d P_m - \chi_{m,n}^* (2^{R_{\min}} - 1) \mathbf{H}_n^b \alpha_n |h_{m,n}^f|^2 P_m$.

By multiplying (28) on both sides by $(\mathbf{V}_{m,n}^A)^*$, and substituting (29) into the obtained multiplied equation, we obtain the following equation, i.e.,

$$\mathbf{Y}_{m,n}^* (\mathbf{V}_{m,n}^A)^* = \mathbf{0}. \quad (30)$$

where $\mathbf{Y}_{m,n}^* = \chi_{m,n}^* \mathbf{H}_m^d P_m - \varepsilon_{m,n}^* - \chi_{m,n}^* (2^{R_{\min}} - 1) \mathbf{H}_n^b \alpha_n |h_{m,n}^f|^2 P_m$.

It is noted that, from (30), $\text{Rank}(\mathbf{Y}_{m,n}^*) + \text{Rank}((\mathbf{V}_{m,n}^A)^*) \leq K$. Since the channels are independently distributed, it can be verified that $\text{Rank}(\mathbf{Y}_{m,n}^*)$ is at least $K - 1$. That is to say, $\text{Rank}((\mathbf{V}_{m,n}^A)^*) \leq 1$ should be held. On the other hand, to satisfy the QoS requirements, $(\mathbf{V}_{m,n}^A)^* \neq \mathbf{0}$ should be satisfied (or equivalently, $\text{Rank}((\mathbf{V}_{m,n}^A)^*) \geq 1$). As a result, $\text{Rank}((\mathbf{V}_{m,n}^A)^*) = 1$ satisfies, which can complete the proof.

APPENDIX B PROOF OF THEOREM 2

It is easy to prove the objective function of problem (20) as a monotonically increasing function with respect to P_m and α_n , respectively. Therefore, we can assert that, regardless of which TA is selected, the optimal transmit power of this TA is $P_m^* = P_{\max}$. Besides, according to C_{3-1}^{BF} and C_{4-1}^{BF} , we have the lower bound for P_m , which is expressed as (31). Then, let $\alpha_n = 0$, which yields the minimum required transmit power of the AD when the harvested energy of the BD exactly compensate for its circuit power and no information is backscattered. Thus, we can obtain

$$P_{m,n}^{\min} = \max \left\{ \frac{\Phi_n^{-1}(P_n^C)}{|h_{m,n}^f|^2}, \frac{(2^{R_{\min}} - 1) \sigma_w^2}{\text{Tr}(\mathbf{H}_m^d \mathbf{V}_{m,n}^A)} \right\}. \quad (32)$$

On the other hand, according to C_{3-1}^{BF} , C_{4-1}^{PR} , and C_5 , we have

$$0 \leq \alpha_n \leq \begin{cases} \frac{\text{Tr}(\mathbf{H}_m^d \mathbf{V}_{m,n}^A) P_{\max} - (2^{R_{\min}} - 1) \sigma_w^2}{(2^{R_{\min}} - 1) \text{Tr}(\mathbf{H}_n^b \mathbf{V}_{m,n}^A) |h_{m,n}^f|^2 P_{\max}}, \\ 1 - \frac{\Phi_n^{-1}(P_n^C)}{P_{\max} |h_{m,n}^f|^2}. \end{cases} \quad \forall n. \quad (33)$$

Therefore, depending on its monotonicity, the optimal RC α_n^* can be obtained as (21b). In accordance with the above conclusions, the proof is complete.

APPENDIX C PROOF OF THEOREM 3

Defining $\{\alpha_n(i_{A3}), P_m(i_{A3}), q_n(i_{A3}), \mathbf{v}_{m,n}(i_{A3})\}$ as the i_{A3} -th iteration solution of problems (14), (19), (20), and

$$(\mathbf{v}_{m,n}^B)^* \triangleq \frac{\left(\mathbf{h}_{m,n}(\mathbf{h}_{m,n})^H + \sum_{j=1, j \neq n} \mathbf{h}_{m,j}(\mathbf{h}_{m,j})^H + \frac{\sigma_w^2}{P_m} \mathbf{I}_K \right)^{-1} \mathbf{h}_{m,n}}{\left\| \left(\mathbf{h}_{m,n}(\mathbf{h}_{m,n})^H + \sum_{j=1, j \neq n} \mathbf{h}_{m,j}(\mathbf{h}_{m,j})^H + \frac{\sigma_w^2}{P_m} \mathbf{I}_K \right)^{-1} \mathbf{h}_{m,n} \right\|}, \quad (41)$$

(25), the objective function of problem (12) can be calculated as $t_{\text{In}}(\alpha_n(i_{A3}), P_m(i_{A3}), q_n(i_{A3}), \mathbf{v}_{m,n}(i_{A3})) = \min_{\forall n} R_n^{\text{BD}}(\alpha_n(i_{A3}), P_m(i_{A3}), q_n(i_{A3}), \mathbf{v}_{m,n}(i_{A3}))$. For given $\alpha_n(i_{A3})$, $P_m(i_{A3})$, and $q_n(i_{A3})$, $\mathbf{v}_{m,n}(i_{A3}+1)$ can be obtained by using (15) and **Algorithm 1**. Since problem (19) is convex, thus we have

$$\begin{aligned} t_{\text{In}}(\alpha_n(i_{A3}), P_m(i_{A3}), q_n(i_{A3}), \mathbf{v}_{m,n}(i_{A3}+1)) &\geq \\ t_{\text{In}}(\alpha_n(i_{A3}), P_m(i_{A3}), q_n(i_{A3}), \mathbf{v}_{m,n}(i_{A3})). \end{aligned} \quad (34)$$

Then, for given $q_n(i_{A3})$ and $\mathbf{v}_{m,n}(i_{A3}+1)$, $\alpha_n(i_{A3}+1)$ and $P_m(i_{A3}+1)$ can be obtained based on (21a) and (21b). In view of the linearity of (22), we have

$$\begin{aligned} t_{\text{In}}(\alpha_n(i_{A3}+1), P_m(i_{A3}+1), q_n(i_{A3}), \mathbf{v}_{m,n}(i_{A3}+1)) &\geq \\ t_{\text{In}}(\alpha_n(i_{A3}), P_m(i_{A3}), q_n(i_{A3}), \mathbf{v}_{m,n}(i_{A3})). \end{aligned} \quad (35)$$

Next, for given $\alpha_n(i_{A3}+1)$, $P_m(i_{A3}+1)$, and $\mathbf{v}_{m,n}(i_{A3}+1)$, $q_n(i_{A3}+1)$ can be obtained via **Algorithm 2**. Since problem (25) is also convex, thus we have

$$\begin{aligned} t_{\text{In}}(\alpha_n(i_{A3}+1), P_m(i_{A3}+1), q_n(i_{A3}+1), \mathbf{v}_{m,n}(i_{A3}+1)) &\geq \\ t_{\text{In}}(\alpha_n(i_{A3}), P_m(i_{A3}), q_n(i_{A3}), \mathbf{v}_{m,n}(i_{A3})). \end{aligned} \quad (36)$$

Moreover, since α_n and q_n are bounded by $[0, 1]$ and P_m is bound by P_{max} , the objective value of problem (12) has an upper bound within a finite value. Thus, the proposed algorithm can converge to a stable point and at least a sub-optimal solution for problem (12).

APPENDIX D BENCHMARK ALGORITHMS

A. The algorithm with TDMA

1) *Problem Formulation*: This problem can be obtained from the formulated problem by replacing $\text{Pr}(n)$ with τ_n , where τ_n denotes the transmission time of the n -th BD. Specifically, the optimization problem can be expressed as

$$\begin{aligned} \max_{\beta_m, P_m, \alpha_n, \tau_n, \mathbf{v}_{m,n}} \quad & \min_{\forall n} \tau_n \sum_{m=1}^M \beta_m r_{m,n}^{\text{BD}} \\ \text{s.t. } & C_1, C_4, C_5, C_6, C_7, \\ & C_2^{\text{TD}} : \sum_{n=1}^N \tau_n = 1, \\ & C_3^{\text{TD}} : \sum_{n=1}^N \tau_n R_n^{\text{AD}} \geq R_{\text{min}}. \end{aligned} \quad (37)$$

2) *Algorithm Design*: This problem can be solved with the proposed algorithm, except for the optimization of τ_n . Once the other variables are obtained, τ_n can also be optimized

according to linear programming. The detailed process is omitted.

B. The algorithm with TC

1) *Problem Formulation*: Under this scheme, the achievable throughput of the AD needs to be rewritten as

$$R_N^{\text{AD}} = \sum_{m=1}^M \beta_m \log_2 \left(1 + \frac{|(\mathbf{v}_m^A)^H \mathbf{h}_m^d|^2 P_m}{\sum_{n=1}^N \alpha_n |h_{m,n}^f|^2 |(\mathbf{v}_m^A)^H \mathbf{h}_n^b|^2 P_m + \sigma_w^2} \right). \quad (38)$$

And the achievable throughput of the BD needs to be rewritten as

$$R_n^{\text{BD}} = \sum_{m=1}^M \beta_m \log_2 \left(1 + \frac{\alpha_n |h_{m,n}^f|^2 |(\mathbf{v}_m^B)^H \mathbf{h}_n^b|^2 P_m}{\sum_{j=1, j \neq n} \alpha_j |h_{m,j}^f|^2 |(\mathbf{v}_m^B)^H \mathbf{h}_j^b|^2 P_m + \sigma_w^2} \right). \quad (39)$$

Similarly, the CAP of each BD is not in focus. Accordingly, the optimization problem can be expressed as

$$\begin{aligned} \max_{\beta_m, P_m, \alpha_n, \mathbf{v}_{m,n}, \mathbf{v}_m^A} \quad & \min_{\forall n} R_n^{\text{BD}} \\ \text{s.t. } & C_1, C_4, C_5, C_6, C_7, \\ & C_{3-1}^{\text{FD}} : R_N^{\text{AD}} \geq R_{\text{min}}. \end{aligned} \quad (40)$$

2) *Algorithm Design*: For this problem, the proposed algorithm can still be used after removing the solution for the CAP sub-problem. Besides, the MRC used to solve for the beamforming vector of the backscattering signal in the previous section should be replaced by the MMSE, which can be expressed as (41), where $\mathbf{h}_{m,n} \triangleq \sqrt{\alpha_n} \mathbf{h}_{m,n}^f \mathbf{h}_n^b$. The detailed process is omitted.

REFERENCES

- [1] M. Vaezi *et al.*, "Cellular, wide-area, and non-terrestrial IoT: A survey on 5G advances and the road toward 6G," *IEEE Commun. Surveys Tuts.*, vol. 24, no. 2, pp. 1117–1174, 2nd Quart. 2022.
- [2] Y. Liu *et al.*, "Rethinking sustainable sensing in agricultural Internet of Things: From power supply perspective," *IEEE Wireless Commun.*, vol. 29, no. 4, pp. 102–109, Aug. 2022.
- [3] Y. Liu, D. Li, H. Dai, C. Li and R. Zhang, "Understanding the impact of environmental conditions on zero-power Internet of Things: An experimental evaluation," *IEEE Wireless Commun.*, early access, Oct. 2022. doi: 10.1109/MWC.007.2200177.
- [4] M. Centenaro *et al.*, "A survey on technologies, standards and open challenges in satellite IoT," *IEEE Commun. Surveys Tuts.*, vol. 23, no. 3, pp. 1693–1720, 3rd Quart. 2021.
- [5] Y. Xu *et al.*, "Joint computation offloading and radio resource allocation in MEC-based wireless-powered backscatter communication networks," *IEEE Trans. Veh. Tech.*, vol. 70, no. 6, pp. 6200–6205, Jun. 2021.
- [6] J. -P. Niu and G. Y. Li, "An overview on backscatter communications," *J. Commun. Inf. Netw.*, vol. 4, no. 2, pp. 1–14, Jun. 2019.
- [7] N. Van Huynh *et al.*, "Ambient backscatter communications: A contemporary survey," *IEEE Commun. Surveys Tuts.*, vol. 20, no. 4, pp. 2889–2922, 4th Quart. 2018.

- [8] D. Darsena, "Noncoherent detection for ambient backscatter communication systems over OFDM signals," *IEEE Access*, vol. 7, pp. 159415–159425, Oct. 2019.
- [9] D. Li, H. Zhang, and L. Fan, "Adaptive mode selection for backscatter assisted communication systems with opportunistic SIC," *IEEE Trans. Veh. Tech.*, vol. 69, no. 2, pp. 2327–2331, Feb. 2020.
- [10] B. Gu *et al.*, "Many a little makes a mickle: Probing backscattering energy recycling for backscatter communications," *IEEE Trans. Veh. Tech.*, vol. 72, no. 1, pp. 1343–1348, Jan. 2023.
- [11] Y. Xu *et al.*, "Robust energy-efficient optimization for secure wireless-powered backscatter communications with a non-linear EH model," *IEEE Commun. Lett.*, vol. 25, no. 10, pp. 3209–3213, Oct. 2021.
- [12] Y. Zhang, B. Li, F. Gao, and Z. Han, "A robust design for ultra reliable ambient backscatter communication systems," *IEEE Internet Things J.*, vol. 6, no. 5, pp. 8989–8999, Oct. 2019.
- [13] D. Li and Y.-C. Liang, "Price-based bandwidth allocation for backscatter communication with bandwidth constraints," *IEEE Trans. Wireless Commun.*, vol. 18, no. 11, pp. 5170–5180, Nov., 2019.
- [14] D. Li, "Capacity of backscatter communication with frequency shift in Rician fading channels," *IEEE Wireless Commun. Lett.*, vol. 8, no. 6, pp. 1639–1643, Dec. 2019.
- [15] P. Zhang *et al.*, "Enabling practical backscatter communication for onbody sensors," in *Proc. ACM SIGCOMM*, pp. 370–383, Aug. 2016.
- [16] D. Li, "Two birds with one stone: Exploiting decode-and-forward relaying for opportunistic ambient backscattering," *IEEE Trans. Commun.*, vol. 68, no. 3, pp. 1405–1416, Mar. 2020.
- [17] D. Li, "Hybrid active and passive antenna selection for backscatter-assisted MISO systems," *IEEE Trans. Commun.*, vol. 68, no. 11, pp. 7258–7269, Nov. 2020.
- [18] Y. Ye *et al.*, "Delay minimization in wireless powered mobile edge computing with hybrid BackCom and AT," *IEEE Wireless Commun. Lett.*, vol. 10, no. 7, pp. 1532–1536, Jul. 2021.
- [19] X. Kang, Y. -C. Liang, and J. Yang, "Riding on the primary: A new spectrum sharing paradigm for wireless-powered IoT devices," *IEEE Trans. Wireless Commun.*, vol. 17, no. 9, pp. 6335–6347, Sept. 2018.
- [20] D. Li, "Backscatter communication via harvest-then-transmit relaying," *IEEE Trans. Veh. Tech.*, vol. 69, no. 6, pp. 6843–6847, Jun. 2020.
- [21] D. Li, "Backscatter communication powered by selective relaying," *IEEE Trans. Veh. Tech.*, vol. 69, no. 11, pp. 14037–14042, Nov. 2020.
- [22] J. Yu *et al.*, "Stabilizing frame slotted aloha-based IoT systems: A geometric ergodicity perspective," *IEEE J. Selected Areas Commun.*, vol. 39, no. 3, pp. 714–725, Mar. 2021.
- [23] Y. -C. Huang *et al.*, "Iterative collision resolution for Slotted ALOHA with NOMA for heterogeneous devices," *IEEE Trans. Commun.*, vol. 69, no. 5, pp. 2948–2961, May 2021.
- [24] Z. Hadzi-Velkov, S. Pejoski, R. Schober, and N. Zlatanov, "Wireless powered ALOHA networks with UAV-mounted-base stations," *IEEE Wireless Commun. Lett.*, vol. 9, no. 1, pp. 56–60, Jan. 2020.
- [25] B. Zhao, G. Ren, X. Dong, and H. Zhang, "Optimal irregular repetition slotted ALOHA under total transmit power constraint in IoT-oriented satellite networks," *IEEE InternetThings J.*, vol. 7, no. 10, pp. 10465–10474, Oct. 2020.
- [26] A. Iqbal and T. -J. Lee, "Spatiotemporal medium access control for wireless powered IoT networks," *IEEE Internet Things J.*, vol. 8, no. 19, pp. 14822–14834, Oct. 2021.
- [27] H.-H. Choi and W. Shin, "Slotted ALOHA for wireless powered communication networks," *IEEE Access*, vol. 6, pp. 53342–53355, Sept. 2018.
- [28] Z. Hadzi-Velkov, S. Pejoski, N. Zlatanov, and R. Schober, "Proportional fairness in ALOHA networks with RF energy harvesting," *IEEE Wireless Commun. Lett.*, vol. 8, no. 1, pp. 277–280, Feb. 2019.
- [29] Y. Li and K. -W. Chin, "Random channel access protocols for SIC enabled energy harvesting IoTs networks," *IEEE Systems J.*, vol. 15, no. 2, pp. 2269–2280, Jun. 2021.
- [30] S. Han, Y. -C. Liang, and G. Sun, "The design and optimization of random code assisted multi-BD symbiotic radio system," *IEEE Trans. Wireless Commun.*, vol. 20, no. 8, pp. 5159–5170, Aug. 2021.
- [31] C. Chen, G. Wang, P. D. Diamantoulakis, R. He, G. K. Karagiannidis, and C. Tellambura, "Signal detection and optimal antenna selection for ambient backscatter communications with multi-antenna Tags," *IEEE Trans. Commun.*, vol. 68, no. 1, pp. 466–479, Jan. 2020.
- [32] S. Wang, M. Xia, K. Huang and Y. -C. Wu, "Wirelessly powered two-way communication with nonlinear energy harvesting model: Rate regions under fixed and mobile relay," *IEEE Trans. Wireless Commun.*, vol. 16, no. 12, pp. 8190–8204, Dec. 2017.
- [33] D. Li, W. Peng, and F. Hu, "Capacity of backscatter communication systems with tag selection," *IEEE Trans. Veh. Tech.*, vol. 68, no. 10, pp. 10311–10314, Oct. 2019.
- [34] Y. Zhang, F. Gao, L. Fan, X. Lei, and G. K. Karagiannidis, "Secure communications for multi-tag backscatter systems," *IEEE Wireless Commun. Lett.*, vol. 8, no. 4, pp. 1146–1149, Aug. 2019.
- [35] Z.-Q. Luo, W.-K. Ma, A. M.-C. So, Y. Ye, and S. Zhang, "Semidefinite relaxation of quadratic optimization problems," *IEEE Signal Process. Mag.*, vol. 27, no. 3, pp. 20–34, May 2010.
- [36] S. Boyd and L. Vandenberghe, *Convex Optimization*. Cambridge, U.K.: Cambridge Univ. Press, 2004.
- [37] Y. Ye, *Interior Point Algorithm: Theory and Analysis*. New York: Wiley, 1997.
- [38] M. Grant and S. Boyd. (2008). *CVX: Matlab Software for Disciplined Convex Programming*. [Online]. Available: <http://cvxr.com/cvx>.
- [39] X. Sun *et al.*, "Joint beamforming and power allocation in downlink NOMA multiuser MIMO networks," *IEEE Trans. Wireless Commun.*, vol. 17, no. 8, pp. 5367–5381, Aug. 2018.
- [40] Y. Xu *et al.*, "Resource allocation for secure SWIPT-enabled D2D communications with α fairness," *IEEE Trans. Veh. Tech.*, vol. 71, no. 1, pp. 1101–1106, Jan. 2022.